

Colored semi-transparent Cu-Si oxide thin films prepared by magnetron sputtering

J. Gil-Rosta,^{1,*} F. Yubero,¹ R. Fernández,⁴ T. Vilajoana,² P. Artús,² J. C. Dürsteler,²
J. Cotrino,¹ I. Ortega,³ and A. R. González-Elipe¹

¹Instituto de Ciencia de Materiales de Sevilla (CSIC – U. Sevilla), C/ Américo Vespucio 49, E-41092 Sevilla, Spain

²INDO (Av. Alcalde Barnils), 72. 08174 Sant Cugat del Vallès, Spain

³Centro Nacional de Aceleradores (CSIC-U. Sevilla), Tomas Alba Edison 7, E-41092 Sevilla, Spain

⁴Dept. of Physical Metallurgy, Centro Nacional de Investigaciones Metalúrgicas (CENIM) CSIC, Av. Gregorio del Amo 8, E-28040 Madrid, Spain

*gilrostra@icmse.csic.es

Abstract: Colored semi-transparent Cu-Si oxide thin films have been prepared by reactive magnetron sputtering from a single cathode of copper-silicon composition. Thin films of different composition and optical response were obtained by changing process parameters like the relative amount of copper in the target and the O₂/Ar mixture of the reactive plasma gas. The film characteristics were analyzed by several techniques. Their optical properties (refractive index, absorption coefficient, color) have been correlated with the process parameters used in the film preparation as well as with the film stoichiometry and chemistry.

©2011 Optical Society of America

OCIS codes: (310.6860) Thin films, optical properties; (310.1860) Deposition and fabrication; (310.3840) Materials and process characterization; (330.4460) Ophthalmic optics and devices.

References and links

1. M. Arbab and J. J. Finley, "Glass in architecture," *Int. J. Appl. Glass Sci.* **1**(1), 118–129 (2010).
2. C. M. Parler, J. A. Ritter, and M. D. Amiridis, "Infrared spectroscopic study of sol-gel derived mixed-metal oxides," *J. Non-Cryst. Solids* **279**(2-3), 119–125 (2001).
3. C. Córdoba, R. Arroyo, J. L. G. Fierro, and M. Viniegra, "Study of xerogel-glass transition of CuO/SiO₂," *J. Solid State Chem.* **123**(1), 93–99 (1996).
4. M. G. Ferreira da Silva and J. M. Fernandez-Navarro, "Colour of silicate sol-gel glasses containing CuO," *J. Non-Cryst. Solids* **100**(1-3), 447–452 (1988).
5. B. Balamurugan and B. R. Mehta, "Optical and structural properties of nanocrystalline copper oxide thin films prepared by activated reactive evaporation," *Thin Solid Films* **396**(1-2), 90–96 (2001).
6. A. S. Reddy, G. V. Rao, S. Uthanna, and P. S. Reddy, "Structural and optical studies on dc reactive magnetron sputtered Cu₂O films," *Mater. Lett.* **60**(13-14), 1617–1621 (2006).
7. V. F. Drobný and D. L. Pulfrey, "Properties of reactively-sputtered copper oxide thin films," *Thin Solid Films* **61**(1), 89–98 (1979).
8. P. Carvalho, J. M. Chappé, L. Cunha, S. Lanceros-Méndez, P. Alpuim, F. Vaz, E. Alves, C. Rousselot, J. P. Espinós, and A. R. González-Elipe, "Influence of the chemical and electronic structure on the electrical behavior of zirconium oxynitride films," *J. Appl. Phys.* **103**(10), 104907 (2008).
9. H. L. Smith and A. J. Cohen, "Absorption spectra of cations in alkali-silicate glasses of ultra-violet transmission," *Phys. Chem. Glasses* **4**, 173–187 (1963).
10. I. Nakai, C. Numako, H. Hosono, and K. Yamasaki, "Origin of the red color of satsuma copper-ruby glass as determined by EXAFS and optical absorption spectroscopy," *J. Am. Ceram. Soc.* **82**(3), 689–695 (1999).
11. T. Akai, H. Yamanaka, and H. Wakabayashi, "Preparation of copper-ruby glasses by sputtering: the effect of atmosphere on the growth of copper particles," *J. Am. Ceram. Soc.* **79**(4), 859–864 (1996).
12. C. R. Bamford, "The application of the ligand field theory to coloured glasses," *Phys. Chem. Glasses* **3**, 189–202 (1962).
13. J. F. Ziegler, J. P. Biersack, and U. Littmark, *The Stopping and Range of Ions in Solids* (Pergamon, 1985), Vol. I.
14. J. Schanda, *Colorimetry: Understanding of the CIE System* (John Wiley and Sons, 2007).
15. F. Liu, C. S. Ren, Y. N. Wang, X. L. Qi, and T. C. Ma, "The optical emission spectroscopy study of an rf-plasma-enhanced magnetron sputtering system," *Vacuum* **81**(3), 221–225 (2006).
16. F. Gracia, F. Yubero, J. P. Holgado, J. P. Espinós, A. R. González-Elipe, and T. Girardeau, "SiO₂/TiO₂ thin films with variable refractive index prepared by ion beam induced and plasma enhanced chemical vapor deposition," *Thin Solid Films* **500**(1-2), 19–26 (2006).
17. G. Papadimitropoulos, N. Vourdas, V. Vamvakas, and D. Davazoglou, "Optical and structural properties of copper oxide thin films grown by oxidation of metal layers," *Thin Solid Films* **515**(4), 2428–2432 (2006).

18. B. Lefez, R. Souchet, K. Kartouni, and M. Lenglet, "Infrared reflection study of CuO in thin oxide films," *Thin Solid Films* **268**(1-2), 45–48 (1995).
19. M. Scrocco, "Satellite structure in the x-ray photoelectron spectra of CuO Cu₂O," *Chem. Phys. Lett.* **63**(1), 52–56 (1979).
20. J. P. Espinós, J. Morales, A. Barranco, A. Caballero, J. P. Holgado, and A. R. González-Elipe, "Interface effects for Cu, CuO, and Cu₂O deposited on SiO₂ and ZrO₂: XPS determination of the valence state of copper in Cu/SiO₂ and Cu/ZrO₂ catalysts," *J. Phys. Chem. B* **106**(27), 6921–6929 (2002).
21. C. D. Wagner, "Chemical shifts of Auger lines, and the Auger parameter," *Faraday Discuss. Chem. Soc.* **60**, 291–300 (1975).
22. G. Moretti, "Auger parameter and Wagner plot in the characterization of chemical states by X-ray photoelectron spectroscopy: a review," *J. Electron Spectrosc. Relat. Phenom.* **95**(2-3), 95–144 (1998).
23. J. Morales, J. P. Espinós, A. Caballero, A. R. González-Elipe, and J. A. Mejías, "XPS study of interface and ligand effects in supported Cu₂O and CuO nanometric particles," *J. Phys. Chem. B* **109**(16), 7758–7765 (2005).
24. A. Forouhi and I. Bloomer, "Optical dispersion relations for amorphous semiconductors and amorphous dielectrics," *Phys. Rev. B* **34**(10), 7018–7026 (1986).
25. A. E. Rakhshani, "Measurement of dispersion in electrodeposited Cu₂O," *J. Appl. Phys.* **62**(4), 1528–1529 (1987).
26. T. Mahalingam, J. S. P. Chitra, S. Rajendran, M. Jayachandran, and M. J. Chockalingam, "Galvanostatic deposition and characterization of cuprous oxide thin films," *J. Cryst. Growth* **216**(1-4), 304–310 (2000).
27. A. Parretta, M. K. Jayaraj, A. Di Nocera, S. Loreti, L. Quercia, and A. Agati, "Electrical and optical properties of copper oxide films prepared by reactive RF magnetron sputtering," *Phys. Status Solidi A* **155**(2), 399–404 (1996).
28. J. Pierson, E. Duverger, and G. Banakh, "Experimental and theoretical contributions to the determination of optical properties of synthetic paramelaconite," *J. Solid State Chem.* **180**(3), 968–973 (2007).
29. C. R. Bamford, "The application of the ligand field theory to coloured glasses," *Phys. Chem. Glasses* **3**, 189–202 (1962).
30. R. Fernandez-Serrano, A. Vilajoana-Mas, J. C. Dürsteler-López, J. Gil-Rostra, F. Yubero-Valencia, A. R. González-Elipe, "Polymer lens comprising a hardening layer, and absorbent layer, and a interferential multilayer and corresponding method," PCT/ES2010/000100.
31. F. J. Ferrer, F. Yubero, J. A. Mejías, F. J. García-López, and A. R. González-Elipe, "Microscopic and macroscopic dielectric description of mixed oxide thin films," *J. Appl. Phys.* **102**(8), 084112 (2007).
32. F. Yubero, A. Stabel, and A. R. González-Elipe, "Optical properties and electron spectroscopy characterization of Al_xTi_{1-x}O₂ thin films," *J. Vac. Sci. Technol. A* **16**(6), 3477–3482 (1998).

1. Introduction

Colored thin films have been prepared by a variety of methods including physical vapor evaporation, magnetron sputtering or plasma enhanced chemical vapour deposition (PECVD) [1–7]. In most cases, the films not only present a given color but also a certain glow because of the highly reflecting character of their surfaces. In many cases, these thin films also present a good electrical conductivity. Within this type of materials we can quote the nitrides, oxinitrides, carbides and nitrocarbides of the elements of the first transition series [8]. In comparison with the huge number of works on this topic available in the literature, there are very few reports on the preparation of colored oxide thin films which show some absorption in the visible region of the electromagnetic spectra. These films can find application in important industrial sectors related to decorative coatings or ophthalmic industry due to their aesthetic aspect and other functional properties.

A typical way to tailor the optical properties of oxide thin film materials, particularly their color, is to adjust the relative concentration of two single oxides mixed in a single phase. The range of variation of the optical characteristics of the films achieved in this way can be very wide if the two oxides mixed together have rather different refractive index and extinction coefficient. This idea is related to the common use of transition metal oxides to color glasses, traditionally employed in stained-glass windows and other hand-craft glasses [3,4,9–12].

However, control of the optical performance (refractive index, absorption, color) in thin films of reduced thickness faces important problems related with the adjustment of the concentration of the coloring cation and the tuning of their chemistry, particularly if the deposition process occurs at low temperature and no post-deposition treatment is feasible because of the thermal stability of the substrate. For example, this is the case for ophthalmic and other optical applications based on polymeric lenses. In this regard, it is particularly convenient that the colored cation to be incorporated is fully compatible with SiO₂ or other

transparent oxides used as standard low index materials in antireflective or dielectric mirror coatings or as antiscratching coatings.

In this paper, we report on semi-transparent coatings based on mixed Cu-Si oxide thin films prepared by reactive magnetron sputtering, where copper is the coloring cation and silicon, in 4+ oxidation state, defines the host transparent matrix. The incorporation of copper in silicate glasses is a well known procedure to color them. For example, the characteristic ruby color is achieved by incorporation of metallic Cu colloidal particles in transparent silica or sodium silicate matrix [9,10]. It is also well known that glasses with reddish color can be obtained by the incorporation of Cu^{2+} ions and CuO clusters in these transparent matrices [3,4,9,12]. Thus, a crucial important point for the characterization of the prepared Cu-Si oxide thin films has been to distinguish whether the constituent oxides form a randomly distributed mixed phase (solid solution of the oxide phases) or segregate into separated phases, and to which extent the local electronic structure around the two cations is dependent on mixing. Another important issue from a technological point of view is the in situ control of the deposition process. In this respect, we have characterized the plasma discharge used in the deposition process by Optical Emission Spectroscopy (OES). Special effort has been devoted to correlate the characteristics of the process plasma with the final properties of the films. Finally, information about the local electronic structure of the films has been also gained by means of X-ray Photoelectron Spectroscopy (XPS) and Fourier Transform Infrared (FTIR) spectroscopies.

2. Experimental

2.1 Sample preparation

Mixed Cu-Si oxide thin films were prepared by reactive magnetron sputtering. Silicon targets of 2 inches diameter were used as the source of silicon. Copper was supplied by Cu strips (0.25 mm thickness, 1.4 mm wide from Goodfellow) wrapped to the Si target along its diameter. Samples were prepared with 1, 2, 3 and 5 strips. As evidenced by the erosion track formed in the target, sputtering mainly occurred in a circumference of ~20 mm of radius (i.e., ~125 mm circumference length). The area ratio of the sputtered copper strips was about 3, 6, 9, and 15% of the total target area for the experimental situations used for the preparation of the films. At industrial scale this approach could be substituted by one in which targets of Si-Cu alloys or mixtures are used to assure automatic reproducibility of results. Samples with different optical performances were also prepared by varying the O_2/Ar ratio in the process gas mixture. The O_2/Ar gas mixture was set with mass flow controllers. The oxygen mass flow Φ_{O_2} was varied between 4 to 25 sccm, while the argon mass flow Φ_{Ar} was varied between 40 and 10 sccm. Thus, the mass flow ratio $\Phi_{\text{O}_2}/\Phi_{\text{Ar}}$ was varied between 0.1 and 2.5. The base pressure in the deposition chamber was 2×10^{-6} mbar and the working pressure was set constant to 5×10^{-3} mbar. The magnetron head (GENCOA, 5 cm diameter targets) was powered with a pulsed DC source (MPS15 from Milko Angelov Consulting Ltd). A pulse frequency of 80 kHz and a duty cycle of 40% were used, with applied powers ranging between 100 and 300 W. The sample holder was polarized with -100 V. The target-sample distance was also varied between 50 to 100 mm. In these conditions, the sample temperature during film growth was always below 373 K.

The reactive plasmas used for deposition of the thin films were characterized by Optical Emission Spectroscopy (OES). The emission spectrum was analyzed using a 0.5 m CVI Digikrom DK480 monochromator (CVI Laser Corporation, Albuquerque, NM), with two 1200 grooves/mm gratings, 200/600 blaze. Wavelength selective filters may be used to eliminate the unwanted radiation. In the experiments, the spectral resolution was of 0.2 nm, and spectral sensitivity ranging from 200 to 900 nm (Hamamatsu R928 phototube). The light was collected by an optical fiber which was fixed to the monochromator and positioned near the middle plane between the anode and the cathode using a vacuum feedthrough with a collimating lens in the plasma chamber.

2.2 Thin film characterization

Thin film microstructure was analyzed with a Hitachi S4800 field emission scanning electron microscopy (SEM). Cross sectional and planar views of thin films prepared on Si(100) wafers were taken to characterize the microstructure and to assess the film thicknesses.

Elemental depth profiling was performed by means of Rutherford Backscattering Spectrometry (RBS) at the 3 MeV tandem ion accelerator of the Centro Nacional de Aceleradores of Seville. The RBS spectra were analyzed with the SRIM software [13].

Chemical characterization by X-ray Photoelectron Spectroscopy (XPS) was carried out with a PHOIBOS 5MCD electron analyzer using unmonochromatised Al-K α radiation. Prior to the XPS characterization a mild O $_2^+$ (1 keV, sample current 1 μ A/cm 2 , 20 min) sputtering was performed to all the samples to remove the adventitious carbon contamination.

Fourier Transform Infrared spectroscopy (FT-IR) in transmission mode was performed in a Nicolet 510 apparatus for thin films prepared on polished undoped Si(100) wafers to identify the type of bonding and local structural arrangement around each metal cation.

Optical characterization of the films was performed by transmission and reflection UV-VIS in a Perkin-Elmer Lambda 12 spectrometer. Refractive index and extinction coefficient were obtained by least squared fit of the simulation of the transmitted and reflected spectra. Color coordinates were evaluated according to standard theory [14].

3. Results

3.1 Analysis of the deposition process

OES analysis of the magnetron plasma discharge has been carried out in situ, during thin film growth, as a function of process parameters. As a general behavior, all emitted lines increase in intensity when the magnetron power is increased. More interesting is the performance for a fixed power. Figure 1 shows a series of OES spectra, recorded in the 315-425 nm range, using a series of standard conditions (fixed magnetron power to 100 W, total pressure to 5×10^{-3} mbar, target-sample distance of 10 cm, and 3 Cu strips in the target and several Φ_{O_2}/Φ_{Ar} ratios) during the deposition processes. The strongest lines in these spectra can be easily ascribed to Cu-I (I_{324} , I_{327}) and Ar-I (I_{416} , I_{420}) emissions [15]. We observe that these emission lines increase in intensity as the amount of Ar in the plasma discharge increases (for fixed power and pressure). The inset in Fig. 1 shows the intensity ratio between these Cu and Ar lines. When $\Phi_{O_2}/\Phi_{Ar} \geq 1$ the ratio between the Cu and Ar emissions I_{Cu}/I_{Ar} ($I_{Cu} = I_{324} + I_{327}$; $I_{Ar} = I_{416} + I_{420}$) remains constant. However, it increases up to a factor 2 for $\Phi_{O_2}/\Phi_{Ar} = 0.1$.

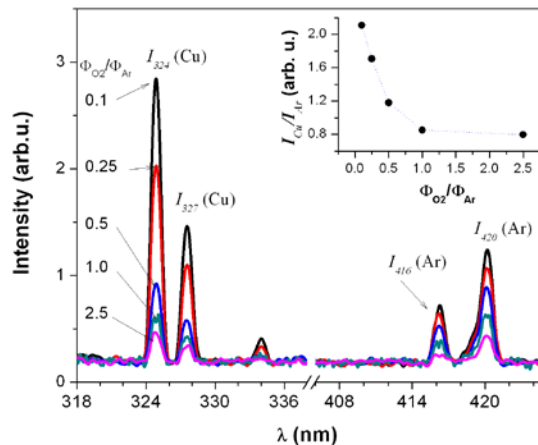


Fig. 1. OES spectra corresponding to several Φ_{O_2}/Φ_{Ar} ratios of the process plasma discharge, as indicated. Bands are assigned to different species according to [15]. Inset: Intensity ratios of the strongest Cu ($I_{324} + I_{327}$) and Ar ($I_{416} + I_{420}$) emission lines in the plasma discharge as a function of the gas flow ratio Φ_{O_2}/Φ_{Ar} corresponding to a Si target with 3 Cu strips, 100 W applied power and 5×10^{-3} mbar total pressure in the reaction chamber.

Regarding the deposition rate d_r , it is found that it diminishes when the sample-target distance increases (5-10 cm range), and increases with the power supplied to the magnetron (100-300 W) and number of Cu strips in the target. For example, for 100 W power, a sample target distance of 10 cm, and $\Phi_{O_2}/\Phi_{Ar} = 1.0$, d_r increases from 3.2 nm/min for no Cu strip (deposition of pure SiO_2) to 5.2 nm/min for 5 strips. It also varies with the mass flow ratio Φ_{O_2}/Φ_{Ar} used during the deposition process. Thus, for 100 W, 10 cm sample-target distance and 3 Cu strips, it increases from 3.8 nm/min to 9.8 nm/min when Φ_{O_2}/Φ_{Ar} decreases from 2.5 to 0.1. Table 1 collects a survey of preparation conditions and the corresponding deposition rates.

3.2 Elemental composition and depth analysis

The in-depth composition of the films was studied by RBS. Figure 2 shows typical RBS in-depth composition spectra and their fitting with the SRIM software. The analysis demonstrates that, in all cases, copper distributes homogeneously in depth and that the copper content varies depending on the deposition conditions. Besides, no significant surface segregation of any of the two constituent cation is observed. Table 1 summarizes the relative stoichiometry x_{Cu} ($x_{Cu} = [Cu]/([Si] + [Cu])$), obtained for several preparation conditions. The reported values show that the Cu content in the films is clearly dependent on the number of Cu strips wrapped to the Si target, varying between 0.16, 0.39, and 0.68 when using 1, 3 and 5 Cu strips wrapped to the Si cathode, respectively. On the other hand, x_{Cu} is not significantly affected by Φ_{O_2}/Φ_{Ar} .

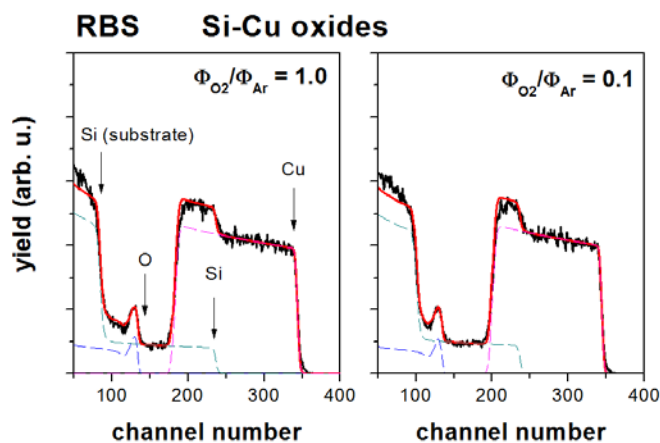


Fig. 2. Experimental and fitted RBS spectra of two selected mixed Cu-Si oxide thin films. The spectra demonstrate a homogenous in-depth distribution of Cu and Si atoms.

The surface composition of the samples was also analyzed by standard XPS. General XPS spectra showed that all the films prepared were composed of O, Si and Cu and very low amount of C atoms (below 2 atomic percent), probably due to adventitious carbon. Regarding the relative x_{Cu} values defined above, both XPS and RBS techniques agreed in the quantification within 5 atomic %, thus confirming that no surface segregation of any of the constituents was present.

3.3 Microstructure and bonding structure of the films

Figure 3 shows typical SEM cross section images obtained for the Si-Cu oxide films. They appear flat and featureless, without any defined grain structure. The structure of the films was also assessed by means of standard Bragg-Brentano X-ray diffraction analysis. No diffraction reflections were detected, confirming the amorphous character of the structure of the films.

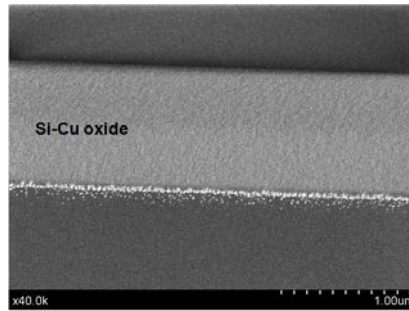


Fig. 3. SEM cross section micrograph of a typical Cu-Si oxide thin film.

Information about the bonding environment around Si and Cu atoms was obtained by FT-IR analysis. Figure 4 shows a series of FT-IR spectra of selected samples. We observe that the stretching mode corresponding to Si-O-Si vibration, that appears at about 1065 cm^{-1} for pure SiO_2 films, shifts to lower wavenumbers (to $\sim 1055\text{ cm}^{-1}$) as the amount of Cu in the film increases. At the same time a new band at $\sim 925\text{ cm}^{-1}$ develops in the spectra. This latter band is a clear indication of Si-O-Cu bond formation [16]. For films with 50% Cu the Si-O-Si band has nearly disappeared, indicating that there is no segregation of a pure SiO_2 phase in the films. Note also that a broad band at about $450\text{-}650\text{ cm}^{-1}$ develops when the amount of Cu in the films increases. However, the typical bands to Cu-O-Cu stretching modes in either Cu_2O (at 615 cm^{-1}) or CuO (480 and 529 cm^{-1}) are not observed in the spectra [17,18]. This confirms the absence of any significant phase segregation of these oxides, and therefore that the films can be described as a solid solution of silicon and copper oxides.

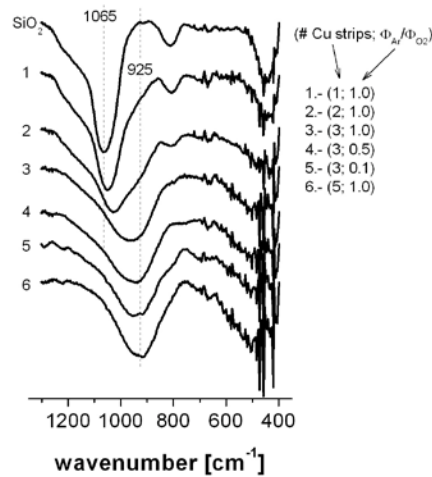


Fig. 4. FT-IR spectra of a series of Cu-Si oxide thin films with increasing number of Cu strips in the Si cathode and prepared with 3 strips and increasing values of $\Phi_{\text{O}_2}/\Phi_{\text{Ar}}$ for the process gas.

3.4 Chemical state analysis and local bonding structure

Figure 5 shows a series of Cu $2p$ spectra obtained for several Cu-Si mixed oxide samples. The evolution in the shape of the spectra can be rationalized by a progressive change in the relative content of copper atoms with either Cu^+ or Cu^{2+} oxidation states [19,20]. We observe that it varies from a situation with mostly Cu^{2+} for films prepared with one copper strip and $\Phi_{\text{O}_2}/\Phi_{\text{Ar}} = 1.0$ to pure Cu^+ for the films prepared with three copper strips and $\Phi_{\text{O}_2}/\Phi_{\text{Ar}} = 0.1$

(i.e., the minimum amount of O₂ in the reactive gas that warrants full oxidation of silicon to Si⁴⁺). The partition between these two oxidation states can be deduced by linear combination of the spectra of corresponding to pure Cu²⁺ and Cu⁺ states. The [Cu⁺]/([Cu⁺] + [Cu²⁺]) ratios obtained in this way are reported in Table 1 for the different preparation conditions. In general we obtain that, for a fixed Cu content in the Cu-Si target, the amount of copper atoms in the Cu + oxidation state which are incorporated in the Cu-Si mixed oxide thin film increases for lower Φ_{O₂}/Φ_{Ar} ratios. However, precise quantification of the film chemistry based only on this technique has to be taken with care, since we have observed that the surface cleaning procedure (mild O₂⁺ sputtering) tends to reduce the Cu²⁺ species to Cu⁺ at the sample surface.

Table 1. Survey of Experimental Conditions and Properties Obtained for Mixed Si-Cu Oxides Prepared by Reactive Magnetron Sputtering

# Cu strips	Φ _{O₂} /Φ _{Ar} (sccm)	<i>d_r</i> (nm/min)	[Cu]/([Cu] + [Si])	[Cu ⁺]/([Cu ⁺] + [Cu ²⁺])	<i>n</i> ₅₅₀	<i>k</i> ₅₅₀
0	10/10	13	0	-	1.46	<0.005
1	10/10	18	0.16	0	1.64	0.020
2	10/10	24	0.27	0.20	1.76	0.030
3	10/10	27	0.39	0.35	1.83	0.062
5	10/10	35	0.68	0.48	2.12	0.15
3	4/40	7	0.38	1	1.81	0.063
3	25/10	25	0.40	0.36	1.82	0.058

Further information of the chemical nature and local electronic structure around the two constituent cations of the mixed oxide thin films can be gained through the Si and Cu Auger parameters [21–23]. The Auger parameter is a local probe that can be correlated to: i) changes in the chemical nature (i.e., oxidation state) of the emitter atom and ii) variation in the extra-atomic relaxation energy when, for a fixed oxidation state, the local environment of a cation changes.

Auger parameters of Si α_{Si} and Cu α_{Cu} have been evaluated in the usual way [21,22]

$$\alpha_{\text{Si}} = \text{BE}(\text{Si } 2p) + \text{KE}(\text{Si KLL})$$

$$\alpha_{\text{Cu}} = \text{BE}(\text{Cu } 2p_{3/2}) + \text{KE}(\text{Cu L}_3\text{VV})$$

where BE(Si 2*p*) and BE(Cu 2*p*_{3/2}) are the binding energies of the Si 2*p* and Cu 2*p*_{3/2} signals and KE(Si KLL) and KE(Cu L₃VV) are the kinetic energies of the Si KLL and Cu L₃VV Auger emissions, respectively.

Figure 6 (left) shows that α_{Si} varies linearly between 1712.2 to 1712.6 eV as the Cu percentage increases in the Si-Cu-O matrix. As a reference, the α_{Si} of pure SiO₂ samples (prepared without Cu) appears at 1711.4 eV. Note that for all studied samples, silicon atoms are always present as Si⁴⁺ species. Therefore, the increase of α_{Si} as the amount of Cu in the films increases indicates that the photoholes created at the Si sites relax easier (more energy is released by polarization of the nearby matrix) as the amount of copper in the films increases. Therefore, the probability that Cu is the second neighbor through the development of Si-O-Cu bond structures increases with increasing Cu content in the films. This result points again to lack of phase segregation, yielding as a result a continuous evolution in the Auger parameter of Si⁴⁺ species from the pure SiO₂ matrix to Si diluted in a mostly CuO_x matrix for the samples with highest x_{Cu} values.

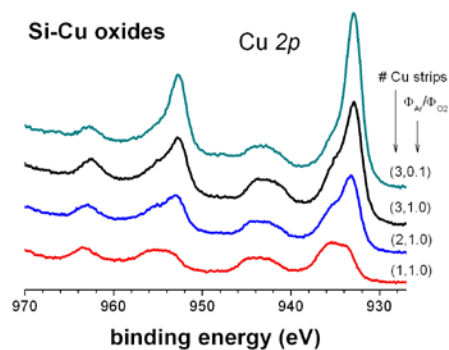


Fig. 5. Cu 2p photoemission spectra of Cu-Si oxide thin films prepared with different experimental process parameters.

The opposite behavior is observed for α_{Cu} . The interpretation of the evolution of α_{Cu} with the films composition is not so straightforward, as both the oxidation state (Cu^+ , Cu^{2+}) and the polarization effects vary simultaneously. Figure 6 (right) shows the evolution of α_{Cu} with the relative amount of Cu^+ species in the samples, as determined by XPS. Since the reported Auger parameter of Cu^+ species in Cu_2O is 1849.2 eV and Cu^{2+} species in CuO is 1851.6 eV (see Fig. 6 (right)), it is likely that changes in α_{Cu} are a consequence of both the presence of different oxidation states in the films and the influence of the different polarization of the environment [20].

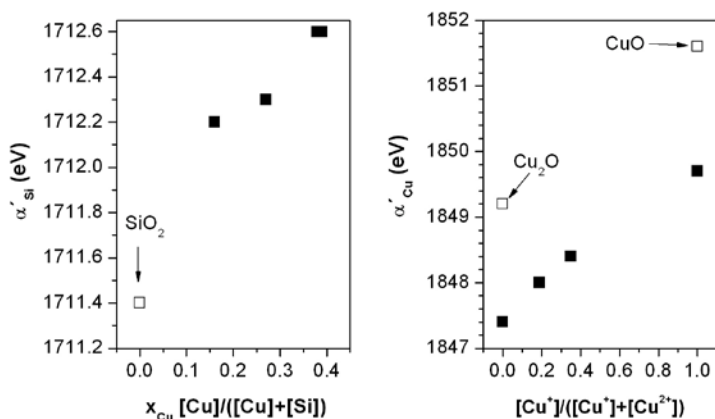


Fig. 6. Silicon Auger parameter α_{Si} (left) and Cu Auger parameters α_{Cu} (right) as a function of the composition of the Cu-Si oxide thin films.

3.5 Optical properties

Figure 7 shows transmission UV-Vis spectra of several films prepared on glass with 100 watts as magnetron power. It shows a series of spectra of samples prepared with a fixed ratio $\Phi_{O_2}/\Phi_{Ar} = 1.0$ and varying the number of Cu strips wrapped to the target, as well as spectra of samples prepared with several Cu strips and different mass flow ratio Φ_{O_2}/Φ_{Ar} . The thicknesses of these samples are about 0.2 microns. It is apparent that the overall absorption of the films increases with the number of Cu strips in the cathode and for lower Φ_{O_2}/Φ_{Ar} values, i.e., with the percentage of Cu in the films (see Table 1). It is observed a constant weak

absorption above 0.6 microns. This absorption increases for shorter wavelengths. The threshold at about 0.3 microns corresponds to the absorption of the glass used in this study.

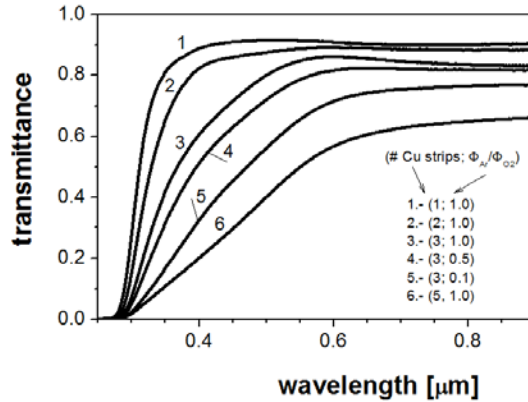


Fig. 7. UV-Vis transmission spectra of a series of Cu-Si oxide thin films prepared under several preparation conditions (see legend).

The refractive index and extinction coefficient of Cu-Si oxide materials was evaluated by simulation of transmission and reflection UV-Vis spectra of the films, considering a homogeneous single layer and a Forouhi-Bloomer model of the complex refractive index [24]. The results of this analysis for the series of samples shown in Fig. 7 is reported in Fig. 8. Refractive index of pure SiO₂ (prepared without Cu strips and $\Phi_{O_2}/\Phi_{Ar} = 1.0$) is also included for completeness. Table 1 collects the refractive index values at 550 nm (n_{550}) for these films. It is found that the refractive index of the Cu-Si oxide films increases with the Cu content in the films. Thus, for $\Phi_{O_2}/\Phi_{Ar} = 1.0$ and $x_{Cu} = 0.16, 0.27, 0.37,$ and 0.68 we obtain that $n_{550} = 1.64, 1.76, 1.83,$ and $2.12,$ respectively. Besides, for a fixed Cu/Si stoichiometry, it is found that lowering the Φ_{O_2}/Φ_{Ar} ratio, the refractive index further increases. According to the previous chemical quantification, this increase of refractive index is correlated with the increase of Cu⁺ species in the films.

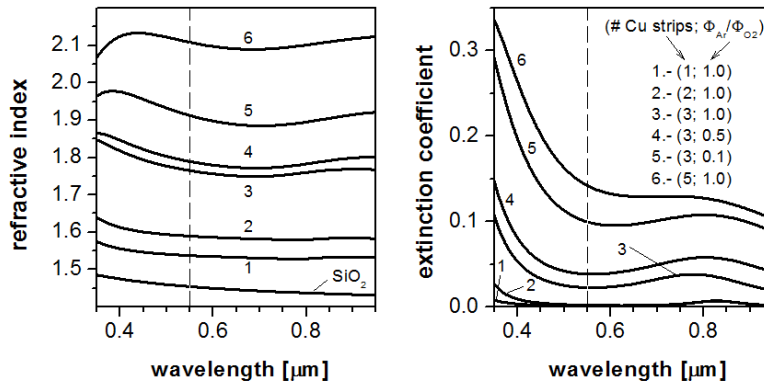


Fig. 8. Refractive index (left) and extinction coefficient (right) of a series of Cu-Si oxide thin films for a Φ_{O_2}/Φ_{Ar} ratio of 1.0 and different number of strips in the cathode and for 3 stripes and different values of the Φ_{O_2}/Φ_{Ar} ratio.

At this point it is convenient to correlate the obtained results with data reported in the literature for single SiO₂, Cu₂O or CuO oxides. It is well known that the refractive index of SiO₂ is about 1.45. Refractive indices of cuprous oxide thin films [6,17,18,25–27], cupric oxide [17,18,27] and mixtures of them [28] have been reported in the literature. From the

rather broad dispersion of reported values, a reasonable n_{550} of the cuprous oxide is about 2.6, while a slightly lower value can be assumed for cupric oxide. These results are consistent with the values obtained in our study. The highest values of refractive index 2.12 was obtained for the $x_{Cu} = 0.7$.

On the other hand, the extinction coefficient increases as the percentage of Cu in the films increases. Note that, besides an increase of intensity and energy shift to longer wavelengths of the main absorption edge, it was necessary to include a wide localized absorption band at about 750 nm to achieve satisfactory fitting of the UV-Vis spectra. This absorption band has been previously ascribed to Cu^{2+} in CuO [29]. The previous considerations are also valid for the description of the absorption coefficient of the films, a magnitude that gives a more intuitive idea of the light attenuation through them. Figure 9 shows the absorption coefficient determined for a series of films. It increases with the amount of copper in the films and for lower Φ_{O_2}/Φ_{Ar} ratios.

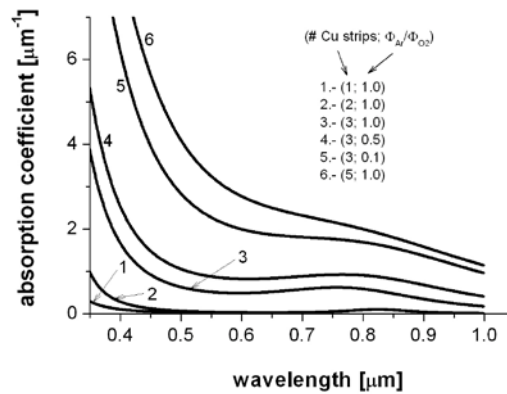


Fig. 9. Absorption coefficient of a series of Cu-Si oxide thin films for an Φ_{O_2}/Φ_{Ar} ratio of 1.0 and different number of stripes in the cathode and for 3 strips and different values of the Φ_{O_2}/Φ_{Ar} ratio.

3.6 Color

As it was mentioned in the introduction section, an application of this kind of films is as decorative coatings, a context where evaluation of their color is a key issue. Color is a perceptual characteristic of light adapted to the human being eye sensitivity. It can be quantified through a colorimetric analysis of a given electromagnetic spectrum. The analysis of the optical properties of the films, according to standard theory of colorimetry [14], can be used to assess their color when considered in transmission.

Figure 10 shows the CIE1931 chromaticity diagram including the (x,y) chromaticity coordinates of the Cu-Si oxide thin films studied in this work. They have been evaluated for transmission geometry of the films deposited on quartz, considering a D65 illuminant, and an observer at 2 degrees field of view. It is found that by increasing the Cu content in the films or their thickness, the color shifts from the achromatic point towards the greenish yellow region (about 570- 580 nm) of the chromaticity diagram. This is due mainly to the absorption induced by the band at about 600-800 nm.

CIE 1931 chromaticity diagram

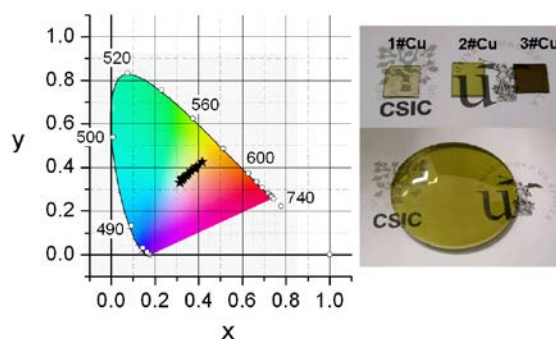


Fig. 10. Left: (x,y) chromaticity coordinates (evaluated in transmission) of the Cu-Si oxide thin films studied in this work represented in the CIE 1931 chromaticity diagram. Right: Example of the deposition of Si-Cu mixed oxides with 1, 2 or 3 Cu strips wrapped to a Si target and $\Phi_{O_2}/\Phi_{Ar} = 0.1$.

Figure 11 shows another representation of the color characteristics of the Cu-Si oxide thin films studied in this work. In this case, the L^* , a^* and b^* color coordinates in the CIELAB color space are shown. The representation of the color coordinates in the CIELAB space is convenient for accurate specification of object colors (two colors which appear similar to a human observer lie close together in the $L^*a^*b^*$ space). Color differences are easily quantified in this space, as they are evaluated as Euclidean distances. The plot includes the evolution of the lightness L^* , and color coordinates a^* and b^* as a function of thickness for 3 particular preparation conditions (3 Cu strips and $\Phi_{O_2}/\Phi_{Ar} = 1.0$ and 0.1 , and 5 strips with $\Phi_{O_2}/\Phi_{Ar} = 1.0$). Note first that L^* decreases as the thickness of the film increases. Besides, note that a^* varies ± 3 units about the value $a^* = 0$. This variation can be justified by the changes induced in the transmitted color due to interference effects. On the other hand, b^* increases steadily as the thickness increases. This behavior corresponds to colors with approximately constant hue (defined as the $\arctan(b^*/a^*)$ and increasing chroma (modulus of the (a^*,b^*) vector), when Cu content and thickness are increased. Other experimental conditions tested in this study showed weaker effects on the color variation.

An important component of the achieved color is due to the absorption band about 700-800 nm. However the actual transmitted color is also modulated by the absorption induced in the rest of the electromagnetic spectrum and the increase of the refractive index with the Cu content in the films.

Owing to the strict control of the optical properties achievable with this kind of films, we have proposed their use as optical coatings for colored ophthalmic lenses [30].

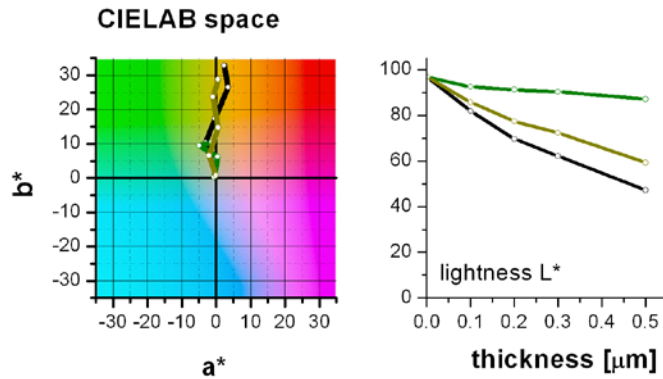


Fig. 11. L^* , a^* , and b^* color coordinates in the CIELAB color space of the Cu-Si oxide thin films studied in this work.

4. Discussion

The use of Cu strips wrapped in the Si target has been demonstrated to be a good approach to prepare Cu-Si oxide thin films with variable and controlled composition. In our system, the erosion track at the Si target induced by the magnetron sputtering was a circumference of ~ 20 mm of radius (i.e., ~ 125 mm circumference length). Taking into account the stoichiometries of the Cu-Si oxide films and that each Cu strip covers about 3 mm of the eroded track, it can be estimated that the Cu sputter efficiency is about 6 times higher than that of the Si target (see Table 1) in agreement with reported sputtering yields of Cu and Si [13]. The higher sputtering yield of copper also explains the observed increase in deposition rate with the number of Cu strips (cf. Table 1).

The evolution of OES line intensities can be correlated with the deposition rate. It is observed that the higher the intensity ratio I_{Cu}/I_{Ar} the higher the deposition rate (compare Fig. 2 with data in Table 1). It also correlates with the chemical nature of the Cu species in the films. Thus, if $I_{Cu}/I_{Ar} \gg 0.8$ a majority Cu^+ species become incorporated in the films. On the other hand, if $I_{Cu}/I_{Ar} \ll 0.8$ mainly Cu^{2+} are incorporated into the film structure. Therefore I_{Cu}/I_{Ar} can be used as an “in-situ” monitoring parameter of the deposition process.

This strict control of the deposition conditions and therefore thin film characteristics has allowed us to tune the optical properties of the films and, in particular, to adjust their color within a certain range of variation. Thus, it has been realized that for the same stoichiometry, an increase in the concentration of Cu^{2+} species slightly turn color from the yellow to the greenish-yellow region of the chromatic diagram. These changes should be linked to a decrease of absorption in the $0.6\text{-}0.7\ \mu\text{m}$ range. Thus, it can be concluded that not only the amount of Cu in the films but also the Cu^+/Cu^{2+} ratio affect the absorption spectrum, and therefore the color of the films.

There is a link between the local effect that shows up in changes in the Auger parameter and the macroscopic variation of the refractive index. The classical theory of dielectrics provides the way to correlate extensive and local dielectric properties of a given material. In particular, the microscopic electronic polarizability α_e measures the ability of the electronic clouds to respond to the local electric fields. In the Lorentz-Lorenz approximation, α_e is considered to be proportional to the $(n^2-1)/(n^2+2)$ function. The main contribution to α_e in mixed oxide systems comes from the oxygen ions of the lattice. Changes in extra-atomic relaxation energy of a cation in an oxide (note that oxygen atoms are always their nearest neighbors) show up as variations of the Auger parameter. In fact, the main mechanism for screening of the photoholes in the final state is the formation of local dipoles in the surrounding medium around the cation. Therefore, it is expected a correlation between the changes in the Auger parameter and the $(n^2-1)/(n^2+2)$ function. This has been the case for

other mixed oxide system (Si-Ti, Si-Zr, Si-Al) as reported previously [30,31]. Our analysis in the present work supports that this correlation, previously used with non-absorbing media [31,32], can be extended to weakly absorbing dielectric materials, as it is the case for the Cu-Si mixed oxide system studied here.

Finally, it is worth noting that the results presented above regarding colored oxide thin films by reactive magnetron sputtering using mixed Cu-Si targets can be easily extrapolated to other systems and that the analysis of the plasma is a good procedure for the “in situ” monitoring of the growth process of mixed oxide thin films.

5. Conclusions

The previous results have shown that colored semi-transparent oxide thin films can be prepared by reactive magnetron sputtering from metal cations of two metals, the first one yielding a transparent oxide (Si in our case) that acts as a host matrix and another a transition metal (Cu in this work) that yields a colored aspect. The films, prepared at temperature below 373 K, are a solid solution of the two constituent cations in a common oxide matrix (as suggested by FT-IR and XPS analysis). They present a different color depending on characteristics of the films such as the relative concentration of the cations and their oxidation state. In this work we have studied the case of Cu-Si oxides thin films. Their optical properties (refractive index, absorption coefficient, gap, color) have been reported. The color range varied within a line of constant hue about the greenish-yellow region of the chromaticity diagram. This variation in color has been related with the thickness, Cu/Si ratio and chemical state of copper in the films. This method to produce semitransparent colored thin films can be considered as a general procedure for the preparation of thin films with other colors by using cations to supply different chromaticity.

Acknowledgments

We thank the Spanish Ministry of Science and Innovation (Cenit ARTDECO CEN-20072014, MAT2010-18447, MAT2010-21228, Consolider FUNCOAT CSD2008-00023) and the Junta de Andalucía (projects P09-TEP5283 and CTS-5189) for financial support.